ELSEVIER

Tectonophysics 333 (2001) 47–59

TECTONOPHYSICS

www.elsevier.com/locate/tecto

Magnetic lineations constraints for the back-arc opening of the Late Neogene South Banda Basin (eastern Indonesia)

F. Hinschberger[a,*], J.-A. Malod[a], J. Dyment[a], C. Honthaas[b], J.-P. Réhault[a], S. Burhanuddin[c]

[a] *UMR 6538 "Domaines océaniques", IUEM, Technopôle Brest-Iroise, 29280 Plouzané, France*
[b] *Laboratoire de Pétrologie, Tour 26-16, Boîte 110, Université Paris VI, 4 place Jussieu, 75252 Paris Cedex 05, France*
[c] *Departemen Teknik Geologi, Universitas Hasanuddin, Ujung Pandang, Indonesia*

Abstract

The South Banda Basin is located within eastern Indonesia near the triple junction between the Eurasian, Pacific and Indo-Australian plates. It is underlain by oceanic crust, but its origin and age were not well established. It has been interpreted as a Mesozoic trapped piece of Indian ocean or as a Cretaceous–Eocene basin related to the Celebes and Sulu basins, but a Neogene back-arc origin was also considered. Recent geochemical and geochronological studies strongly support the latter hypothesis.

In this paper we present a new analysis of the magnetic data from the eastern part of the South Banda Basin, the Damar Basin. We used magnetic field measurements collected during nine oceanographic cruises from various institutions. Looking for magnetic correlation in the time span given from recent geochronological data, the comparison between measured profiles and theoretical profiles deduced from the reversals of Earth's magnetic field during Neogene time allows us to infer an opening of South Banda Basin during Late Miocene–Early Pliocene time, from 6.5 to 3.5 Ma. Magnetic lineations 2An, 2Ar, 3n, 3r, 3An and possibly 3Ar are recognized, with an extinct spreading centre trending ENE–WSW. At least five segments are identified, each segment being separated by inactive transform faults perpendicular to the extinct spreading centre. A half spreading rate of about 3 cm/yr is calculated, based on spacing of magnetic lineations.

The opening history of the basin is discussed. The cause of cessation of spreading is likely the arc-continent collision dated at about 3 Ma. However the onset of opening is less determined. We suggest that Damar Basin began to open at about 6.5 Ma during magnetic period 3An as an intra-arc basin, separating the Banda volcanic arc to the south from the incipient Lucipara volcanic arc to the north. The latter was probably created at the beginning of rifting of Damar Basin, as shown by both magnetic and geochronological data.

The young age of the South Banda Sea Basin is contradictory with its great depth. We discuss this problem in view of thermal and tectonic considerations. We finally conclude that our magnetic model allows us to more precisely describe the opening of the basin.

Keywords: Banda Sea; Indonesia; back-arc basin; magnetic anomalies

1. Introduction

The South Banda Sea is located in the eastern part of the Indonesian archipelago near a triple junction area between three major plates, namely the Eurasian, Pacific and Indo-Australian plates, which are

* Corresponding author. Fax: +33-02-98-49-87-60.
E-mail addresses: hinsch@sdt.univ-brest.fr (F. Hinschberger), malod@sdt.univ-brest.fr (J.-A. Malod).

0040-1951/01/$ - see front matter
PII: S0040-1951(00)00266-3

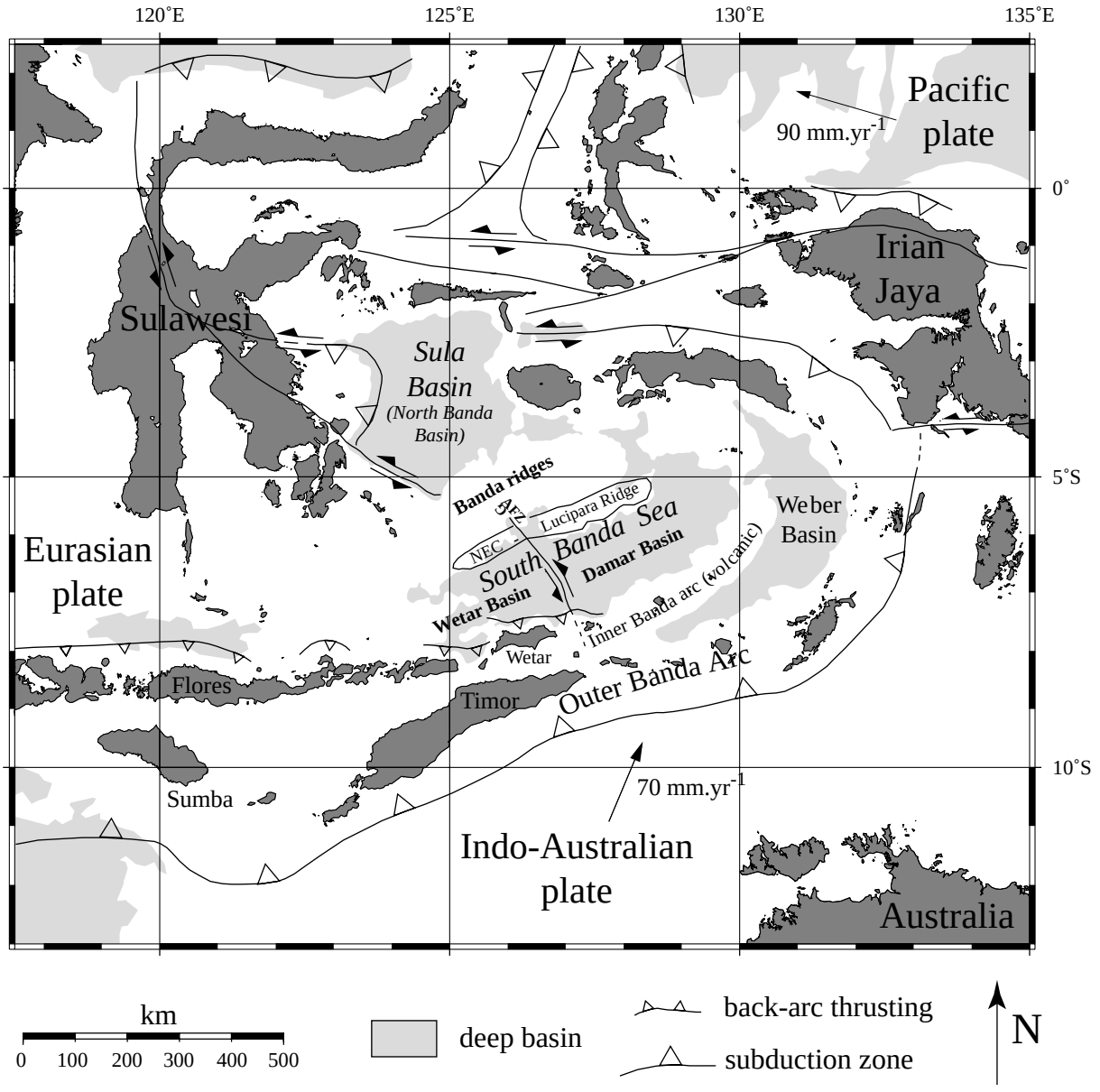

GAFZ: Gunung Api fracture zone

Fig. 1. Location map of Banda Sea region showing the most important structures and basins. Arrows indicate motions of plates relative to Eurasia.

converging since Mesozoic times (Hamilton, 1979; Jolivet et al., 1989, Fig. 1). It is bounded to the south by the inner Banda volcanic arc resulting from the northward subduction of the Indo-Australian plate under the South Banda arc (Hamilton, 1979; Hutchison, 1981; Vroon et al., 1993), and to the north by a submarine volcanic and continental ridge: the Nieuwerkerk-Emperor of China (NEC)–Lucipara

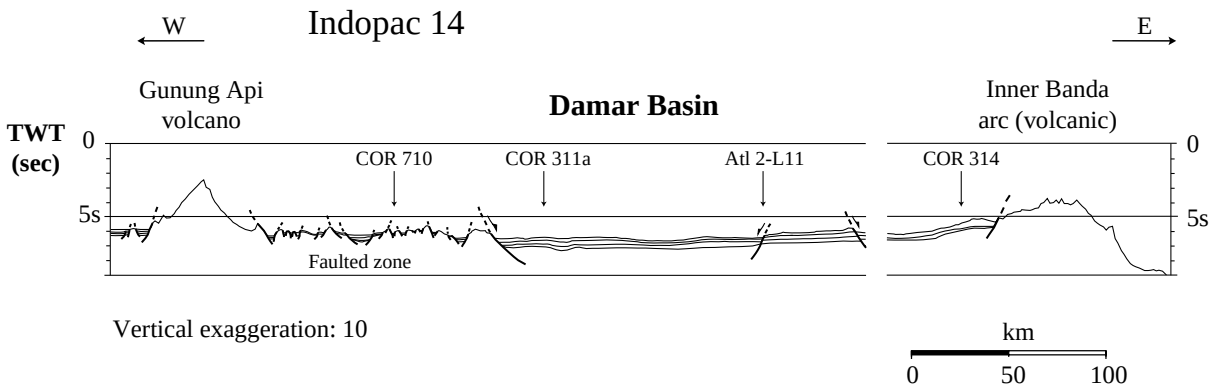

Fig. 2. Seismic profile Indopac 14 along Damar Basin, showing the irregular basement topography in the western part of the basin. See Fig. 3 for location.

Ridge. This ridge forms the southern limit of the Banda ridges that separate the South Banda Basin from the Sula Basin (or North Banda Basin), opened during Late Miocene time (Réhault et al., 1994; Honthaas et al., 1998).

The South Banda Basin exhibits an elongated shape with ENE–WSW direction, parallel to the Banda arc. It is 800 km long and 150 km wide. It can be divided into two parts separated by the Gunung Api fracture zone: the Wetar Basin to the west is 4500 m deep, with a sedimentary cover 1–2 km thick, and numerous seamounts outcropping from the seafloor. To the east the Damar Basin is 5000 m deep, its sedimentary cover rarely exceeds 800 m and no major seamounts are present. Moreover, the Damar Basin exhibits an irregular basement topography in its western part (Fig. 2).

The oceanic nature of the South Banda Basin is well established from seismic refraction and gravity data (Purdy and Detrick, 1978; Bowin et al., 1980). However, its origin and age were long controversial. Both low heat flow values and depth of basement greater than 4500 m are in agreement with a creation of the oceanic crust during Mesozoic or Early Cenozoic time. Moreover, three previous studies based on different interpretations of magnetic lineations identified in the Banda Sea support this hypothesis. Magnetic anomalies as old as 130 Ma (M 13) to 120 Ma (M 8) trending N55°E to N70°E were recognized in the South Banda Basin, which was considered as a Mesozoic trapped piece of the Indian Ocean (Lapouille et al., 1985). Using the same data, Karta (1985) identified magnetic anomalies M 10 to M 0 in the South Banda Basin, with an extinct spreading centre located south of the Banda ridges. In both cases however, Mesozoic magnetic anomalies were also detected on the Lucipara Ridge to the north, where volcanic activity occurred during Late Neogene time (Honthaas et al., 1998), making the hypothesis of a trapped Mesozoic origin for the Banda Sea uncertain. Finally, Lee and McCabe (1986) suggested that the Banda Basin could be a Cretaceous–Eocene basin related to the Celebes and Sulu basins. However, their identifications of magnetic lineations in the South Banda Basin were established using only five magnetic profiles, making these lineations hazardous.

Alternatively, based on geodynamic interpretation of the surrounding islands and forelands, the South Banda Sea was interpreted as a Neogene back-arc Basin related to the South Banda subduction zone (Hamilton, 1979; Nishimura and Suparka, 1990; Villeneuve et al., 1998).

The debate concerning the age and origin of the South Banda Basin was recently closed by the studies of Honthaas et al. (1998). Using geochemical and geochronological data from the Banda volcanic arc and the NEC-Lucipara Ridge, they showed that the South Banda Basin opened by intra-arc spreading during Late Miocene–Early Pliocene time. In this hypothesis, the Wetar segment of the Banda volcanic arc to the south and the NEC–Lucipara Ridge to the north represented a single volcanic arc 8–7 Ma ago. Indeed, both volcanic arcs present strong geochemical affinities and their corresponding calc-alkaline

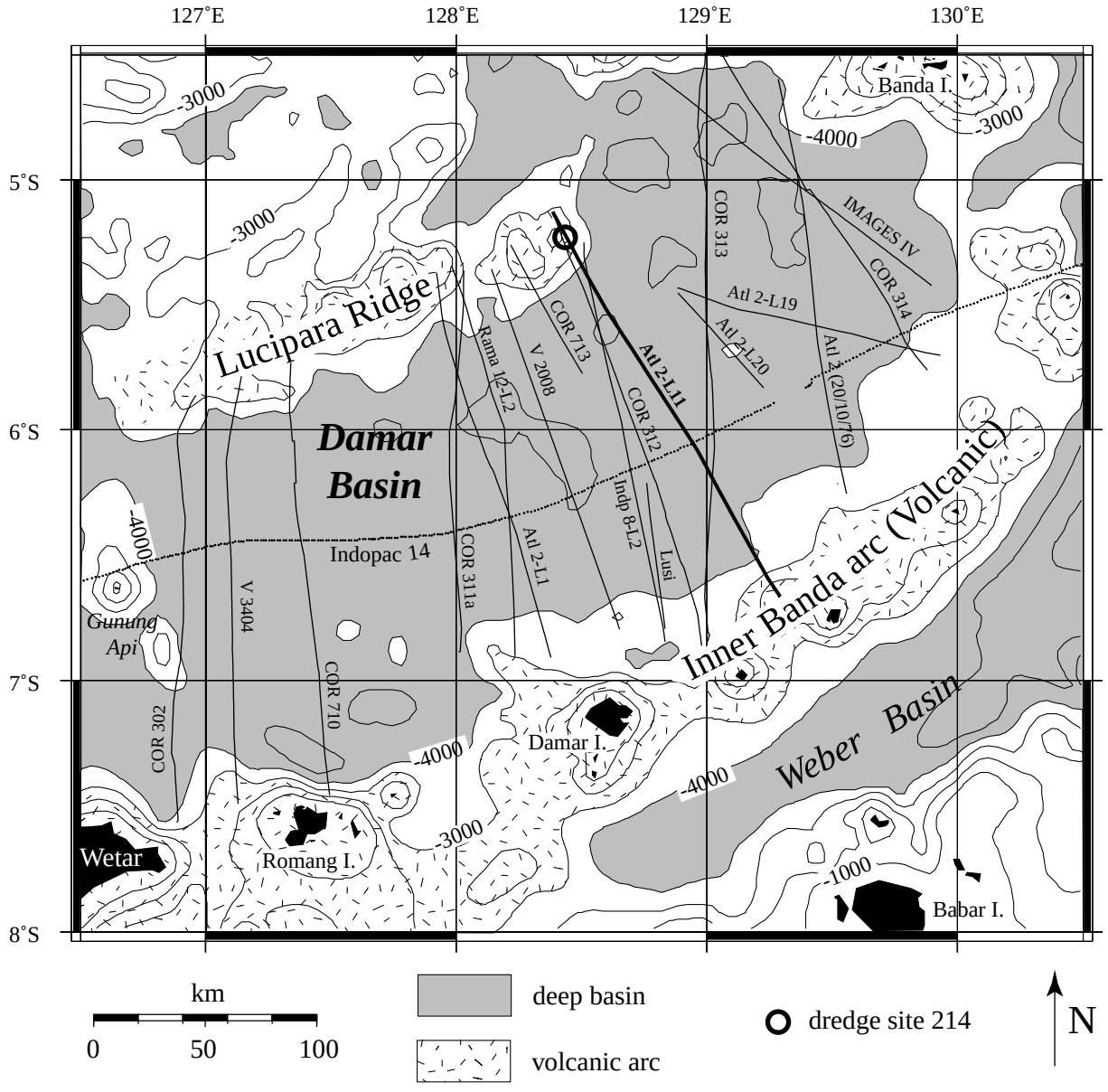

Fig. 3. Map of the magnetic profiles in the Damar Basin. Profile Atlantis 2-L11 is indicated with dark line. Seismic profile Indopac 14 is also located (dotted line). Bathymetry is indicated with 1000 m contour interval.

activity was related to the high dip subduction of the Indian oceanic lithosphere beneath continental blocks originated from New Guinea (Silver et al., 1985). The rifting of the South Banda Basin at about 6 Ma separated the Wetar segment of the Banda volcanic arc to the south from the NEC–Lucipara volcanic arc to the north, and intra-arc opening processes occurred from about 6 to 3 Ma in the Wetar and Damar basins. Finally, volcanic activities stopped at 3 Ma in both volcanic arcs.

Considering this now well-constrained datations of the South Banda Basin opening, we present here a

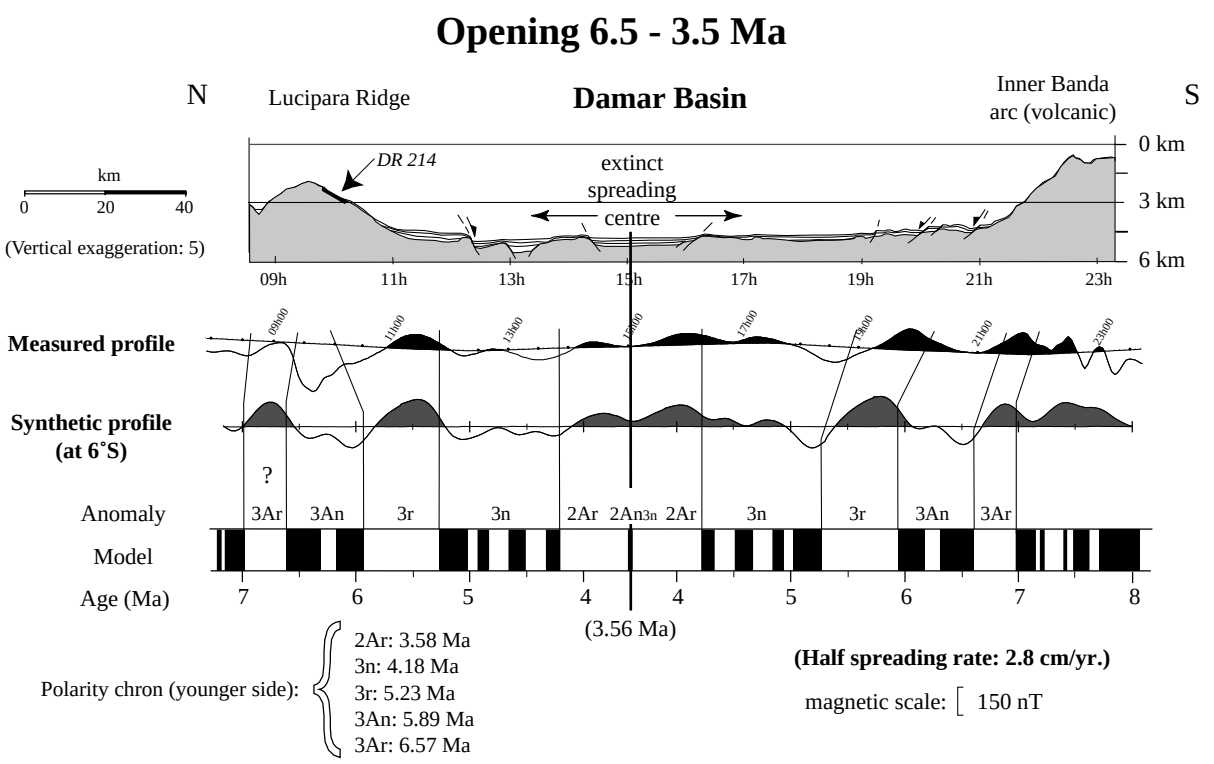

Fig. 4. Identification of the magnetic anomalies by correlation of the profile Atlantis 2-L11 to a synthetic profile. Seismic line L11 is also represented. See Fig. 3 for location.

new synthesis of geological and geophysical data in the basin. The short length of profiles makes difficult any interpretation of magnetic anomalies and does not allow clear determination of the magnetic time scale without other age-constraining data. This can explain the great variety of previous magnetic interpretations. However, if we take into account the precise time span given by geochronological data, we are able to propose a new magnetic correlation in the Damar Basin.

2. Presentation of magnetic data in the Damar Basin

Magnetic anomalies lineations are observed in the two parts of the South Banda Basin. However, higher amplitude anomalies have been correlated with the presence of volcanic seamounts in the middle part of the Wetar Basin, making determination of magnetic lineations impossible. Therefore we focus our study on the Damar Basin, where few seamounts are present.

The location of the magnetic profiles used in the Damar Basin is indicated in Fig. 3. Ten profiles recorded during six oceanographic cruises are available from the NGDC: Lusi 6 (1962), Vema 20-08 (1964), A20-93 of R/V Atlantis 2 (1976) (Fig. 4), Indopac 8 (1976), Vema 34-04 (1977) and Rama 12 (1981). In addition, six profiles from two cruises carried out by ORSTOM are also used (Corindon cruises in 1981 and 1982). Most recently, cruise “Images IV” onboard the R/V Marion Dufresne (1998) provided a magnetic profile across the north-eastern part of Damar Basin. Magnetic data were reduced to magnetic anomalies using the IGRF models (IAGA Division V working group 8, 1996). No correction was applied for the daily solar quiet variation, which does not exceed a few tens of nanoteslas and would not significantly affect the morphology of the studied anomalies. Indeed,

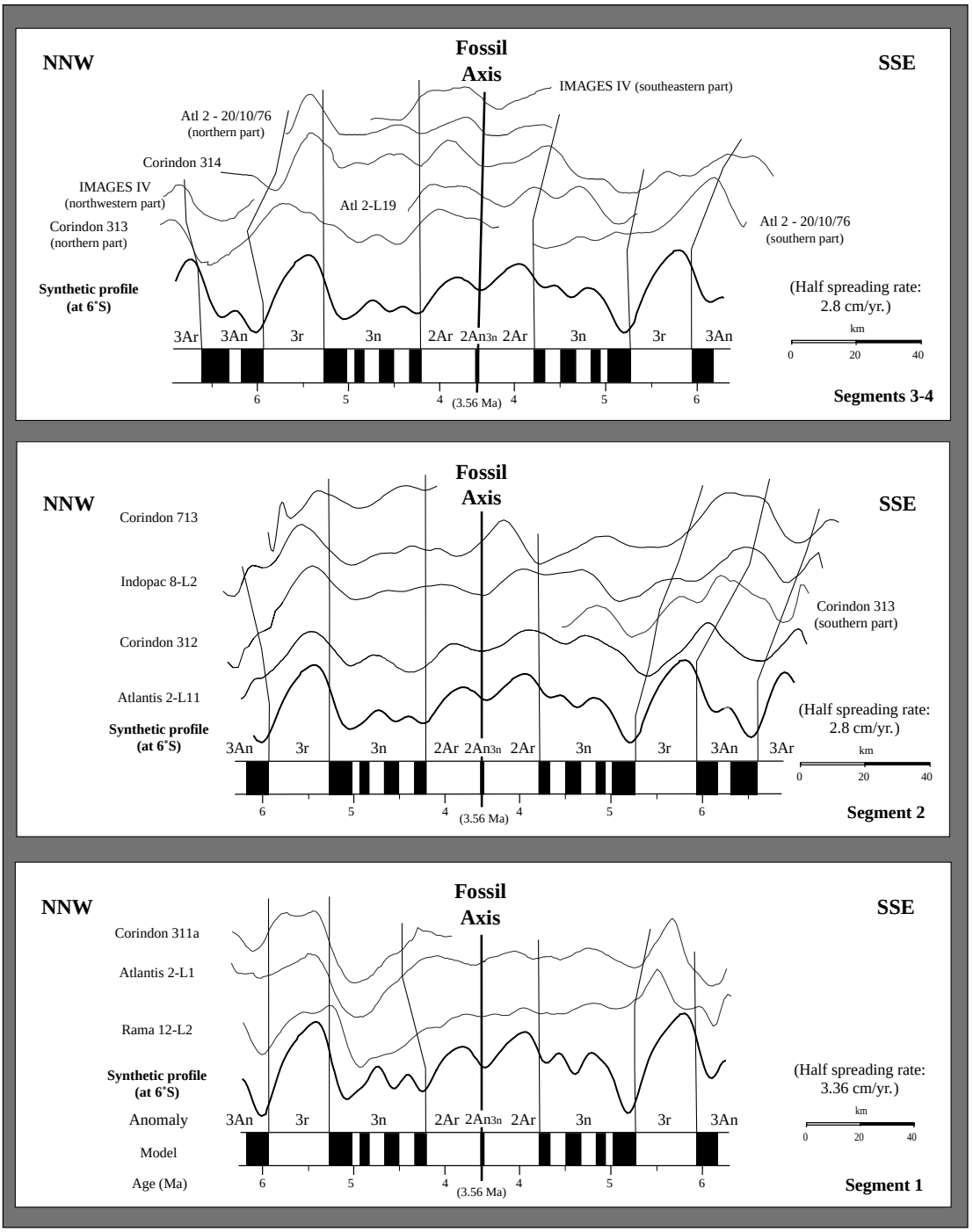

Polarity chron (younger side):
- 2Ar: 3.58 Ma
- 3n: 4.18 Ma
- 3r: 5.23 Ma
- 3An: 5.89 Ma
- 3Ar: 6.57 Ma

magnetic scale: 150 nT

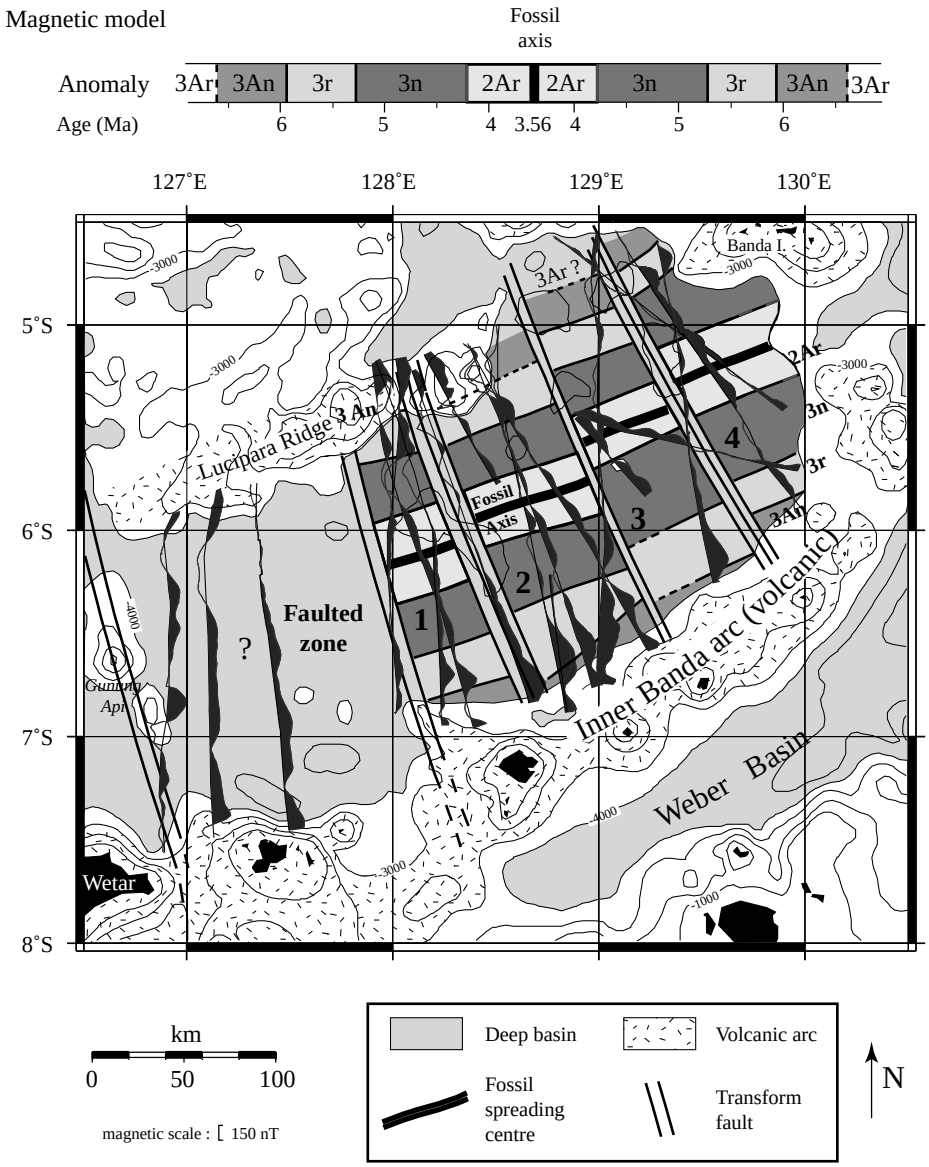

Fig. 6. Map of magnetic anomalies and lineations in the Damar Basin. The magnetic anomalies are represented along the ship's track with the positive part of the variations on the northern or eastern side of the tracks (grey shaded area) and the negative part on the southern or western side. Names of profiles are indicated in Fig. 3.

considering the speed of the ship, the wavelength of fictitious anomalies which could be associated with this daily variation is much longer than that of studied anomalies (Lapouille et al., 1985). It is worth noting that the magnetic equator is at about 10°N at the longitude considered and the study area is not subject to the strong magnetic variations associated to the equatorial electrojet.

Fig. 5. Identification of the magnetic anomalies in the Damar Basin. (Short sections of profiles are not represented, but they are mapped in Fig. 6.)

The resulting 18 profiles across the Damar Basin are used to draw magnetic lineations (Figs. 5 and 6). All profiles are perpendicular to the elongated shape of the basin and are well oriented to depict the ENE–WSW-trending magnetic lineations. The magnetic anomalies display wavelengths of about 20 km and low amplitudes, generally lower than 150 nT (Fig. 5). The low amplitudes are explained by the great depth of the basin (5000 m) and the relative proximity of the magnetic equator. However, amplitudes higher than 200 nT are found at the northern and southern boundaries of the basin. Magnetic anomalies are clearly aligned in an ENE–WSW direction in the middle and eastern parts of the Damar Basin, whereas in the western part no clear defined lineation is observed (Fig. 6).

3. Identification of magnetic anomalies and age of the seafloor of the Damar Basin

As a first step, we examine an extensive set of magnetic anomaly models generated with various spreading rates and times of spreading onset and cessation within Late Neogene time. We assume a 500 m-thick magnetized layer whose top lies 5500 m below sea level, the average depth of the oceanic basement in the Damar Basin. Magnetization is set to ± 10 A/m. The geomagnetic polarity time-scale of Cande and Kent (1995) is used throughout this study. We consider that the South Banda Basin opened in a direction approximately perpendicular to its present elongated shape along a N160°E direction (fossil spreading axis oriented N70°E) and at a latitude close to its present one. Many synthetic profiles were computed using spreading time ranging from Late Miocene to Present, in accord with the time span given by geochemical and geochronological data (Honthaas et al., 1998). Each synthetic profile was compared to the observed anomalies in the Damar Basin.

The best solution corresponds to an opening of the Damar Basin during Late Miocene–Early Pliocene time, from 6.5 to 3.5 Ma, with a symmetric half spreading rate of 2.8 cm/yr. This model is represented in Fig. 4. Since the oceanic crust was created and is observed near the magnetic equator, normal and reverse periods are characterized by negative and positive anomalies, respectively. Comparison of the synthetic profile with measured profile Atlantis 2-L11, which shows well-defined anomalies (Fig. 4), emphasizes their very good similitude.

We identify Late Miocene and Early Pliocene magnetic anomalies 3Ar, 3An, 3r, 3n, 2Ar and 2An3n on each side of the extinct spreading centre, which is located slightly north from the axis of the basin. Our model suggests that spreading in the Damar Basin stopped at about 3.5 Ma, at the beginning of 2An normal period, whereas the basin began to open at about 6.5 Ma. However, magnetic anomalies seem to continue at some place outward, below the Banda volcanic arc to the south (magnetic anomaly 3Ar) and below Lucipara volcanic arc to the north (magnetic anomalies 3An and possibly 3Ar).

Attempts to correlate the resulting synthetic profile have been extended to all the other magnetic profiles available in the Damar Basin (Figs. 5 and 6). This allows us to divide the basin into at least five segments separated by four fossil transform faults. We discuss the correlation for each segment below.

3.1. Central segment (segment 2)

Only three profiles are crossing the entire segment (Atlantis 2-L11, already discussed; COR 312 and Indopac 8-L2, see Figs. 5 and 6). Three other profiles cross parts of this segment (COR 313, COR 713 and Lusi).

This segment is characterized by well-defined magnetic anomalies, which draw magnetic lineations striking in an ENE–WSW direction, parallel to the elongated shape of the basin (Fig. 6). The magnetic lineation interpreted as anomaly 3An is located outside of the basin, on the Lucipara Ridge. To the southeast, profile COR 313 shows anomalies 3n to 3Ar in continuity with those on the neighbouring profile Atlantis 2-L11, indicating that the southernmost part of the profile belongs to the central segment (Figs. 5 and 6). However, magnetic anomalies 2Ar and 2An3n are shifted 20 km northward, and a zone of smooth anomalies appears between the two parts of profile COR 313. We interpret this offset as the trace of a fossil transform fault running NNW–SSE east of the central segment and roughly perpendicular to the extinct spreading centre (Fig. 6).

To the west, profile V 2008 shows subdued anomalies

that do not correlate with our model. Since magnetic lineations are recognized to the west (see below, segment 1) and because this profile is striking NNW–SSE, we propose that it is running along a fossil transform zone constituting the western limit of the central segment (Fig. 6).

3.2. Western segment (segment 1)

Three profiles are located in this segment, which is therefore poorly constrained (Rama 12-L2, Atlantis 2-L1 and COR 311a, see Figs. 5 and 6). These profiles do not show well-defined anomalies, but the major ones, especially 3n and 3r, are preserved, allowing us to draw magnetic lineations parallel to those of the central segment, but shifted about 10 km towards the south (Fig. 6). This offset can be explained by the presence of a NNW–SSE fossil transform fault separating segments 1 and 2 and located along profile V 2008 as proposed above.

Segment 1 is characterized by an opening rate slightly faster than in the central segment (half spreading rate of 3.36 cm/yr instead of 2.80 cm/yr, see Fig. 5). South of the fossil axis, profile COR 311a does not show magnetic anomalies that could be correlated with theoretical profile. We therefore infer another fossil transform fault which constitutes the western limit of the segment. Due to the lack of magnetic profile west of profile COR 311a, the orientation of this fracture zone is unconstrained but its trend is probably parallel to the previous ones (Fig. 6).

We did not try to identify magnetic anomalies in the western part of the Damar Basin, because only three profiles are available there (Fig. 6). Moreover, the oceanic basement is heavily faulted in this region, as seen in Fig. 2. This tectonized zone may result from the juxtaposition of two or more transform faults. Westward the Gunung Api volcanic ridge is the major active structure of the South Banda Basin. It trends NNW–SSE, parallel to transform faults in the Damar Basin (Fig. 6). This structure is likely a transform fault that was active during opening of the South Banda Sea and has been reactivated as a left-hand strike-slip fault since the arc-continent collision took place in Pliocene time.

3.3. Eastern segments (segments 3 and 4)

These two segments are located in the eastern part of Damar Basin and are cut by the following profiles: Atlantis 2 (L20, L19 and 20/10/76 Line); northern part of COR 313; COR 314 and IMAGES IV (Figs. 5 and 6). Comparison of these profiles with the synthetic one reveals the same magnetic lineations, with a half spreading rate of 2.8 cm/yr similar to that of the central segment.

Profile COR 314, located in the easternmost part of the basin, is affected by a long wavelength, likely due to diurnal variations, which superimposes to the anomalies and does not prevent correlation with the synthetic profile (Fig. 5). In the western part of segment 3, a small seamount seen on profile Atlantis 2-L20 has no major effect on the magnetic data. In the northern part of profiles COR 313 and IMAGES IV, magnetic anomaly 3An and possibly magnetic anomaly 3Ar are identified (Figs. 5 and 6).

Segment 3 is limited to the west by a fossil transform fault that separates it from the central segment. To the east, a 10 km offset of the magnetic lineations and fossil axis indicates the presence of a fossil transform fault trending NNW–SSE, which separates segment 3 from segment 4 (Fig. 6). Magnetic profiles Atlantis 2-L19 and Atlantis 2 (20/10/76) cut across this transform fault and show no correlation with synthetic anomalies in their central part.

Segment 4 is bounded to the east by the eastern part of the Banda volcanic arc (Fig. 6). This part of the arc may therefore have been emplaced on a previous transform direction after the South Banda Sea opening.

4. Discussion

Detailed investigation on magnetic anomalies shows that the Damar Basin is divided into at least five segments separated by four fossil transform faults (Fig. 6). The segments are 40–60 km wide and transform faults show 10–20 km left-lateral apparent offsets. The fossil spreading axis is located in the middle part of the basin and trends N70°E, allowing oceanic spreading in a N160°E direction. This direction is in good agreement with the orientation of fossil transform faults, which are nearly perpendicular to the spreading centre. Our magnetic anomaly identifications imply symmetrical spreading with a mean rate of about 3 cm/yr during the opening of the whole

basin. This intermediate rate is not surprising if we consider the Damar Basin as a back-arc or intra-arc basin. Magnetic data in the Damar Basin date the onset of spreading during Late Miocene time at about 6.5 Ma. The timing of opening of the basin is discussed below.

Magnetic anomaly 3Ar (7.0–6.6 Ma) is the oldest magnetic anomaly possibly recognized in the Damar Basin. The observed positive magnetic anomaly resulting from this reverse magnetic field period can be interpreted in two ways. First, in the northern part of segment 3, in a region where the great water depth indicates the occurrence of oceanic crust, it may be associated to oceanic spreading (Figs. 5 and 6). Second, on the northern flank of the Lucipara Ridge, it may more likely result from the emplacement of volcanic bodies (Figs. 4 and 5). Anomaly 3Ar can also be recognized in the northern side of the Banda volcanic arc (Figs. 4 and 5). As for the Lucipara Ridge, we suggest that it is explained by subduction-related volcanism which was here active before the opening of the Damar Basin.

Magnetic anomaly 3An (6.6–5.9 Ma) is mapped in the four segments of the basin, both on their northern and southern sides (Figs. 5 and 6). In the northern side of segments 1 and 2, magnetic anomaly 3An is located on the Lucipara volcanic ridge and can hardly be explained by simple oceanic spreading. Dredgings on the Lucipara Ridge indicate a Late Neogene volcanic arc overlying an older crust including volcanic rocks dated at 46 Ma and interpreted as ophiolitic unit (Honthaas et al., 1998). K–Ar ages of volcanic rocks (site 214) located on the eastern part of Lucipara Ridge close to profile Atlantis 2-L11 (Fig. 3), show that magmatic activity occurred during three distinct periods: 6.8–6.2, around 5 and 4–3.45 Ma (Honthaas et al., 1998). The volcanic ridge is characterized by a strong negative magnetic anomaly, which indicates that the volcanic rocks were emplaced principally during normal periods (Fig. 4). We can therefore infer from both geochemical and magnetic data that most of the Lucipara Ridge was built during magnetic period 3An, from 6.6 to 6.2 Ma. The few volcanic products dated at 6.8–6.6 Ma during magnetic period 3Ar may represent only a small percentage of the volcanic rocks and would not affect the negative magnetic signature of the ridge. The juxtaposition of anomaly 3Ar and 3An on the ridge suggests another explanation. From 6.8 to 6.6 Ma magmatic activity was concentrated in the northern part of the ridge giving rise to anomaly 3Ar earlier to migrate southwards between 6.6 and 5.9 Ma giving rise to anomaly 3An (Fig. 4). We also infer that the reactivation of magmatic activity around 5 Ma (normal period 3n) and 4–3.45 Ma (reverse period 2Ar and normal period 2An) did not change in a significant way the negative magnetic signature of the ridge. Indeed, these two phases of volcanism are of less importance than the first one (see Fig. 5 of Honthaas et al., 1998).

In the deep oceanic domain, magnetic anomaly 3An is clearly identified in the southern part of segments 1–2, indicating that oceanic spreading was already active there while the Lucipara Ridge was being built (Figs. 5 and 6). Consequently, seafloor spreading was strongly asymmetric at the onset of opening, producing most oceanic crust south of the spreading centre. In segments 3 and 4, where the Lucipara Ridge does not extend in, spreading may have occurred earlier and more symmetrically. This suggests a possible westwards migration of the spreading axis. The Lucipara Ridge and the Banda volcanic arc were part of the same volcanic arc prior to the opening of the Damar Basin at 6.5 Ma. This is in agreement with the hypothesis developed by Honthaas et al. (1998) concerning the origin of the NEC-Lucipara Ridge and Banda volcanic arc as a single volcanic arc 8–7 Ma ago, which was separated into two parts by the opening of the South Banda back-arc Basin.

Next to magnetic anomaly 3An, magnetic anomalies 3r, 3n, 2Ar and the oldest part of 2An are clearly identified in the four segments, indicating that spreading lasted for about 3 Ma (Fig. 6). Seafloor spreading in the Damar Basin stopped at about 3.5 Ma, during normal period 2An3n. The cessation of spreading in the Damar Basin and more generally in the South Banda Basin can be attributed to the arc-continent collision between Australia and the South Banda arc. This collision is dated at about 3 Ma in Timor, SW of Damar Basin, where it is most evolved (Bowin et al., 1980; Audley-Charles et al., 1988; Hartono, 1990; Nishimura and Suparka, 1990; Richardson and Blundell, 1996; McCaffrey, 1996). The end of magmatic activity on both the Lucipara Ridge and the Wetar segment of the Banda volcanic arc at 3 Ma is also thought to result from the collision of Timor with the Banda arc (Abbott and Chamalaun, 1981).

We focused our study in the Damar Basin, where magnetic lineations are clearly evidenced. By comparison, the Wetar Basin which is located to the west in structural continuity with the Damar Basin likely opened during the same time, as inferred from geochemical data. The significant morphostructural contrast that exists between the Wetar and Damar basins concerning their basement depth, their sedimentary infilling and the presence of seamounts, can be explained by different back-arc processes in both the basins. Indeed, Honthaas et al. (1998) suggest a single-rift-type opening for the Damar Basin, which is clearly evidenced by our magnetic study, whereas the Wetar Basin to the west may have formed by multi-rift-type opening. If this hypothesis is true, then the identification of well-defined magnetic lineations in the Wetar Basin is impossible.

Another point which should be discussed is the abnormal depth in the South Banda Basin regarding its very young age. Indeed, with an average depth basement of 5.5 km, the South Banda Basin is one of the deeper young (age < 10 Ma) back-arc basins in the world. This great depth was often taken as one of the more convincing argument for a Mesozoic or Early Tertiary age of the basin (Bowin et al., 1980; Lapouille et al., 1985; Lee and McCabe, 1986). However, the great depth of the basin can be explained by the following three considerations.

First, it is well known that back-arc basins do not follow the depth versus age curve established by Parsons and Sclater (1977) for the major oceans. On the contrary, Park et al. (1990) showed that young back-arc basins present a variety of the basement depth from shallower to deeper than major oceans of the same age. On the other hand, Kobayashi (1984) from a compilation of the age–depth correlation in the back-arc basins suggested that the depth of the basement in those basins is generally 1000 m deeper than the depth obtained from the age–depth equation for major oceans. This difference can be explained by rapid thermal subsidence due to a more important heat loss in the small basins.

Secondly, the Banda Sea Basin has undergone compression since the subduction of the Australian plate beneath the Banda arc stopped during Late Pliocene–Early Pleistocene time. The end of subduction is documented from sedimentological data in the Timor Trough (Richardson and Blundell, 1996) and stratigraphic studies of the Kai accretionary complex (Charlton et al., 1991). In response to the continuous northward motion of the Australian plate, back-arc thrusting of the Banda Sea Basin occurred north of Wetar (Silver et al., 1983; McCaffrey, 1996). Moreover, GPS data indicate that the South Banda domain has yet been accreted to the Australian plate, transferring the shortening northwards on faults within the back-arc basin and in the Seram Trough (Genrich et al., 1996; Walpersdorf et al., 1998; Rangin et al., 1999). We suggest that the resulting compressive tectonic setting of the South Banda Basin has induced tectonic subsidence which adds to thermal subsidence.

Finally, the South Banda Basin domain is located above two slabs converging at depth: the Banda slab to the south dips northward, whereas the Seram slab to the north dips southwestward. The drag stress in the vicinity of these two downgoing lithospheres may also have increased the tectonic subsidence.

5. Conclusions

We used magnetic profiles to date more precisely the spreading episode during Late Miocene to Early Pliocene as proposed by Honthaas et al. (1998). We conclude that the onset of spreading took place at the beginning of chron 3An (6.6 Ma) and perhaps locally, in segments 3 and 4, a little earlier, at chron 3Ar (7 Ma). The initial phase of spreading was strongly asymmetric in segments 1 and 2, with most of the oceanic crust formed south of the spreading axis, while the Lucipara Ridge to the north was characterized by abundant volcanism resulting in a 3An-like negative magnetic anomaly. Before the onset of spreading, arc volcanism was already active both on Lucipara and Banda arcs during chron 3Ar giving rise to positive magnetic anomalies found on some part of these ridges. The magnetic anomaly pattern may therefore indicate a westward migration of the onset of spreading from segments 3 and 4 (anomaly 3Ar) towards segments 1 and 2 (anomaly 3An). Spreading has continued symmetrically after chron 3An and stopped at chron 2An at about 3.5 Ma probably in relation with the arc–continent collision between Australia and the South Banda arc.

The difficulty to recognize the magnetic anomalies

on the magnetic profiles in more tectonized area (western Damar Basin) or region affected by volcanism (Wetar Basin) precluded us to extend this work to the whole Banda Sea Basin. However, based on the tectonic continuity between the basins and the geochronological results, we propose to extend our interpretation to the whole South Banda Sea. The latter constitutes an outstanding example of a basin opened within a volcanic arc in a general convergent geodynamic context. Analogies can be done with other Late Neogene deep back-arc basins, such as the Tyrrhenian Basin in the Mediterranean Sea.

Acknowledgements

Banda Sea cruises were jointly organized by BPPT, Jakarta, and Geobanda group with the support of the French Ministère des Affaires Etrangères and Total-Indonesia. IMAGES IV cruise was organized by IFRTP under the direction of F. Bassinot, and Corindon cruises were organized by ORSTOM (IRD). We thank J.Y. Royer and G. Jacovetti for their help with magnetic model analyses, and X. Morin for his contribution to IMAGES IV magnetic data processing. We acknowledge J.C. Sibuet and E. Silver who made very useful comments on the manuscript. F.H. is supported by a scholarship from the French Ministry of Education, and our research program is supported by UBO. Maps presented in this paper were made using GMT software (Wessel and Smith, 1995).

References

Abbott, M.J., Chamalaun, F.H., 1981. Geochronology of some Banda arc volcanics. In: Barber, A.J., Wiryosujono, S. (Eds.), The Geology and Tectonics of Eastern Indonesia. Geol. Res. Dev. Cent., Spec. Publ. 2, 253–268.

Audley-Charles, M.G., Ballantyne, P.D., Hall, R., 1988. Mesozoic–Cenozoic rift-drift sequence of Asian fragments from Gondwanaland. Tectonophysics 155, 317–330.

Bowin, C., Purdy, G.M., Johnston, C., Shor, G., Lawver, L., Hartono, H.M.S., Jezek, P., 1980. Arc-continent collision in Banda Sea region. Am. Assoc. Pet. Geol. Bull. 64 (6), 868–915.

Cande, S.C., Kent, D.V., 1995. Revised calibration of the geomagnetic polarity timescale for the Late Cretaceous and Cenozoic. J. Geophys. Res. 100 (B4), 6093–6095.

Charlton, T.R., Kaye, S.J., Samodra, H., Sardjono, 1991. Geology of the Kai Islands: implications for the evolution of the Aru Trough and Weber Basin, Banda Arc, Indonesia. Mar. Pet. Geol. 8, 62–69.

Genrich, J.F., Bock, Y., McCaffrey, R., Calais, E., Stevens, C.W., Subarya, C., 1996. Accretion of the southern Banda arc to the Australian plate margin determined by global positioning system measurements. Tectonics 15 (2), 288–295.

Hamilton, W., 1979. Tectonics of the Indonesian region. US Geol. Surv. Prof. Pap. 1078, 345.

Hartono, H.M.S., 1990. Late Cenozoic tectonic development of the Southeast Asian continental margin in the Banda Sea area. Tectonophysics 181, 267–276.

Honthaas, C., Réhault, J.P., Maury, R.C., Bellon, H., Hémond, C., Malod, J.A., Cornée, J.J., Villeneuve, M., Cotten, J., Burhanuddin, S., Guillou, H., Arnaud, N., 1998. A Neogene back-arc origin for the Banda Sea basins: geochemical and geochronological constraints from the Banda ridges (East Indonesia). Tectonophysics 298, 297–317.

Hutchison, S.C., 1981. Review of the Indonesian volcanic arc. In: Barber, A.J., Wiryosujono, S. (Eds.), The Geology and Tectonics of Eastern Indonesia. Geol. Res. Dev. Cent., Spec. Publ. 2, 65–80.

IAGA Division V Working Group 8, 1996. Revision of the International Geomagnetic Reference Field released. EOS Trans. Am. Geophys. Union 77, 153.

Jolivet, L., Huchon, P., Rangin, C., 1989. Tectonic setting of Western Pacific marginal basins. Tectonophysics 160, 23–47.

Karta, K., 1985. Etude géodynamique de la mer de Banda (Indonésie) par interprétation des données magnétiques et gravimétriques. PhD thesis, Univ. de Bretagne Occidentale, Brest, pp. 177.

Kobayashi, K., 1984. Subsidence of the Shikoku back-arc basin. Tectonophysics 102, 105–117.

Lapouille, A., Haryono, H., Larue, M., Pramumijoyo, S., Lardy, M., 1985. Age and origin of the seafloor of the Banda Sea (Eastern Indonesia). Oceanol. Acta 8 (4), 379–389.

Lee, C.S., McCabe, R., 1986. The Banda–Celebes–Sulu basin: a trapped piece of Cretaceous–Eocene oceanic crust? Nature 322, 51–54.

McCaffrey, R., 1996. Slip partitioning at convergent plate boundaries of SE Asia. In: Hall, R., Blundell, D.J. (Eds.), Tectonic Evolution of Southeast Asia. Geol. Soc. Lond. Spec. Publ. 106, 3–18.

Nishimura, S., Suparka, S., 1990. Tectonics of East Indonesia. Tectonophysics 181, 257–266.

Park, C.-H., Tamaki, K., Kobayashi, K., 1990. Age–depth correlation of the Philippine Sea back-arc basins and other marginal basins in the world. Tectonophysics 181, 351–371.

Parsons, B., Sclater, J.G., 1977. An analysis of the variation of ocean floor bathymetry and heat flow with age. J. Geophys. Res. 82 (5), 803–827.

Purdy, G.M., Detrick, R.S., 1978. A seismic refraction experiment in the central Banda Sea. J. Geophys. Res. 83 (B5), 2247–2257.

Rangin, C., Le Pichon, X., Mazzotti, S., Pubellier, M., Chamot-Rooke, N., Aurelio, M., Walpersdorf, A., Quebral, R., 1999. Plate convergence measured by GPS across the Sundaland/Philippine Sea Plate deformed boundary: the Philippines and eastern Indonesia. Geophys. J. Int. 139, 296–316.

Réhault, J.P., Maury, R.C., Bellon, H., Sarmili, L., Burhanuddin, S.,

Joron, J.L., Cotten, J., Malod, J.A., 1994. La Mer de Banda Nord (Indonésie): un bassin arrière-arc du Miocène supérieur. C. R. Acad. Sci., Paris, Sér. II 318, 969–976.

Richardson, A.N., Blundell, D.J., 1996. Continental collision in the Banda arc. Tectonic Evolution of Southeast Asia, Hall, R., Blundell, D.J. (Eds.). Geol. Soc. Lond. Spec. Publ. 106, 47–60.

Silver, E.A., Reed, D., McCaffrey, R., Joyodiwiryo, Y., 1983. Back arc thrusting in the eastern Sunda arc, Indonesia: a consequence of arc-continent collision. J. Geophys. Res. 88 (B9), 7429–7448.

Silver, E.A., Gill, J.B., Schwartz, D., Prasetyo, H., Duncan, R.A., 1985. Evidence for a submerged and displaced continental borderland, north Banda Sea, Indonesia. Geology 13, 687–691.

Villeneuve, M., Réhault, J.P., Cornée, J.J., Honthaas, C., Gunawan, W., The Geobanda group, 1998. Evolution géodynamique de l'Indonésie orientale, de l'Eocène au Pliocène. C. R. Acad. Sci., Paris 327, 291–302.

Vroon, P.Z., Van Bergen, M.J., White, W.M., Varekamp, J.C., 1993. Sr–Nd–Pb isotope systematics of the Banda Arc, Indonesia: combined subduction and assimilation of continental material. J. Geophys. Res. 98 (12), 22349–22366.

Walpersdorf, A., Vigny, C., Manurung, P., Subarya, C., Sutisna, S., 1998. Determining the Sula block kinematics in the triple junction area in Indonesia by GPS. Geophys. J. Int. 135 (2), 351–361.

Wessel, P., Smith, W.H.F., 1995. New version of the generic mapping tools released. EOS Trans. Am. Geophys. Union 76, 329.